JOURNAL OF PROPULSION AND POWER
Vol. 20, No. 4, July–August 2004

Characterization of a Six-Emitter Colloid Thruster Using a Torsional Balance

M. Gamero-Castaño*
Busek Company, Inc., Natick, Massachusetts 01760

Colloid thruster micropropulsion will be tested in space by the New Millennium Program's Space Technology 7-Disturbance Reduction System mission (NASA). The objective of this program is to develop the technologies required for precision spacecraft position control, with accuracy orders of magnitude better than previously demonstrated. This capability will enhance or enable aggressive scientific programs like the Laser Interferometer Space Antenna and the Micro-Arcsecond X-ray Imaging Mission, which are centerpieces of the NASA Office of Space Science roadmap. The colloid thrusters for the Disturbance Reduction System project must produce thrust in the 2–20 μN range, with a maximum step size of 0.1 μN and a noise figure better than 0.1 $\mu\text{N}/\sqrt{\text{(Hz)}}$ in the 1–30 mHz bandwidth. We have operated a six-emitter electrospray source and directly measured its thrusting properties with a torsional balance. We have demonstrated that this colloid thruster can cover the desired thrust range continuously and has a noise figure below 0.1 $\mu\text{N}/\sqrt{\text{(Hz)}}$ in the 7 mHz–1 Hz bandwidth. Its noise spectrum is likely better than 0.1 $\mu\text{N}/\sqrt{\text{(Hz)}}$ down to 1 mHz, but the intrinsic noise of the balance made it impossible to verify this. In another experiment, we compared thrust measurements obtained with both the torsional balance and the time-of-flight technique and found them to differ within 15%. This result supports the use of the inexpensive time-of-flight technique for measuring the thrust of colloid thruster, when modest accuracy is required.

Nomenclature

f_n	=	natural frequency
In	=	beam current
K	=	propellant electrical conductivity
L	=	flight path of beam
$\dot{m}$	=	mass flow rate
Q	=	propellant flow rate
T	=	thrust
Va	=	acceleration voltage
Vn	=	emitter voltage
γ	=	propellant surface tension
ε	=	propellant dielectric constant
ρ	=	propellant density

Introduction

COLLOID thrusters are electrostatic accelerators of electrospray droplets. Initially developed during the 1960s and early 1970s,[1–3] the interest in this technology has resurfaced as new propulsive applications, for which colloid thrusters are particularly well suited, have emerged. For example, the expected proliferation of microsatellites is associated with more flexible missions requiring attitude control, formation flying, trajectory correction, or orbit deployment, all of which require onboard propulsion. It is recognized that colloid thrusters are one of the few technologies that can deliver both the primary and attitude control propulsion required by microsatellites.[4]

The propulsion capability needed for precision spacecraft position control is the second niche ideal for colloid thrusters. Most applications of this type fall in two groups: drag-free flying and separated spacecraft interferometer missions. Drag-free flying requires the use of thrusters to counterbalance forces such as atmospheric drag in near Earth orbits[5] or solar pressure,[6] so that the spacecraft trajectory is only determined by the gravity field. In the case of separated spacecraft interferometer missions, the position of optics on different spacecrafts must be controlled to a fraction of a wavelength, so that the light collected from different spacecrafts can be combined coherently. In missions working with visible or infrared light, this can be accomplished with a coarse control of the spacecraft position and positioning stages acting on the optics. However, other missions based on x-ray interferometry call for spacecraft position control at the nanometer level,[7] and fine micropropulsion becomes an enabling feature. In general terms, the propulsion system required by these missions (e.g., Disturbance Reduction System, Laser Interferometer Space Antenna, and Micro-Arcsecond X-ray Imaging Mission) must deliver thrust continuously in the microNewton range, have a reduced noise figure, and ample thrusting range with sub-microNewton resolution.

The Disturbance Reduction System project (DRS), chosen by NASA as its New Millennium Program Space Technology 7 demonstration (ST7), is a good example of scientific mission requiring and featuring fine micropropulsion.[6,8] The objective of this program is to develop and test in space technologies for precision spacecraft position control. The mission is based on two novel technologies: gravity reference sensors (GRS) and colloid thrusters. The GRS is essentially a test mass that moves freely inside a chamber, which shields the former from all external forces (mainly solar pressure) other than gravity. The function of the colloid thrusters is to counterbalance external forces on the spacecraft (the GRS chamber is rigidly attached to the spacecraft), so that the relative position between the test mass and the spacecraft is kept constant within some specified tolerance, and the variations of the interaction forces between them are acceptably small so that the test mass follows a trajectory determined only by external gravity within 3×10^{-14} $\text{m/s}^2/\sqrt{\text{(Hz)}}$, in the 1–30 mHz bandwidth. Beside this acceleration noise figure, the position noise of the test mass needs to be better than 1 $\text{nm}/\sqrt{\text{(Hz)}}$, in the same bandwidth. To achieve these goals, the colloid thrusters of the DRS-ST7 program have to generate thrust in the 2–20 μN range, with a maximum step size of 0.1 μN, and a noise figure better than 0.1 $\mu\text{N}/\sqrt{\text{(Hz)}}$ in the 1–30 mHz bandwidth.

The research in this paper is a contribution to the development of the colloid thruster technology for the DRS-ST7 project and feeds on previous research.[9–11] We have characterized the performance of a six-emitter electrospray source, the generator of the beam of charged droplets and thrust, with a torsional balance.[12] Using this apparatus, we have proved the thruster's capacity to yield thrust in the 2.33–12.9 μN range, with a predictability of 0.06 μN, and a noise

Received 15 May 2003; revision received 2 September 2003; accepted for publication 2 February 2003.

*Research Scientist, 11 Tech Circle. Member AIAA.

figure better than 0.1 μN/$\sqrt{}$(Hz) in the 7 mHz–1 Hz bandwidth. We plan to improve our designs and measuring techniques to test the specifications of the DRS-ST7 project down to 1 mHz.

The paper is organized as follows: after this introductory section we will describe the experimental setup; the bulk of the thrust characterization with the torsional balance is presented in the next section; then, we will compare the thrust values obtained with the time-of-flight technique and the torsional balance; and some brief conclusions are given in the last section.

Experimental Setup

The thrust measurements were carried out in the setup sketched in Fig. 1. A cylindrical chamber with a diameter of 0.66 m and a length of 0.77 m was evacuated with a 250 l/s turbomolecular pump backed by a 6.2 l/s mechanical pump. The base pressure of the facility was 0.1 mPa. The chamber sat on a bench rigidly fixed to the floor of the lab. The thrust stand itself was placed on a tray fixed to a sliding door of the chamber. The electrospray source was mounted inside a grounded aluminum box, which also contained a reservoir filled with 1-ethyl-3-methylimidazolium bis(trifluoromethylsulfonyl)imide liquid propellant.[13] The box and its content typically weighed 0.45 kg, and an equivalent counterweight was placed on the other side of the rotating arm. The electrospray source consisted of three different electrodes: a six-needle emitter, an extractor grid, and an accelerator grid.[10] The accelerator grid was grounded, while the outputs of two high-voltage power supplies were connected to the emitter and extractor. The voltage difference between these two electrodes was kept constant (typically at 2 kV) to set stable electrosprays, while the emitter voltage was raised or lowered to change the beam acceleration voltage. The flow rate of the liquid was varied by pressurizing/depressurizing the reservoir containing the propellant through a fine Teflon® line connected to an external pressure regulating system. The Teflon line and the power connections were designed to apply negligible torques in the balance's arm. The beam was directed against a grounded collector plate perpendicular to its axis and used to measure the electrospray current. Several electronic devices (power supplies, amplifiers, electrometers, controllers, a linear displacement sensor reader, etc.) controlled and processed the signals associated with the balance and the colloid thruster, and served as an interface between them and a data-acquisition system, and an oscilloscope.

A detailed description of the torsional balance is given elsewhere.[12] Its design is based on two flexural pivots defining the rotation axis of the balance arm: an optical sensor for measuring the linear displacement of the arm perpendicular to its circular motion, and the use of electrostatic forces for calibration and to implement an active damper. Its resolution is estimated to be better than 0.03 μN, and its accuracy is limited by the accuracy with which linear distance and voltage values, which are the parameters associated with the calibration and the output signal of the balance, can be measured. In the present case, we estimate an accuracy better than 3%. Figure 2 shows a calibration of the balance (the balance is excited with a constant torque, inducing a steady displacement of the balance arms), with all four axes of the graph displaying a relevant parameter: the calibration force and torque, and the output of the linear displacement sensor in volts and microns. Note the linearity between displacement and torque (the electrostatic force is applied with a lever arm of 0.266 m), and the negligible interception of the linear fitting with the y axis, which suggest a good performance of the thrust stand. The slope of the line in Fig. 2 is the only fitting parameter used for the thrust stand measurements and makes it possible to compute the torsional spring rate accurately. The torsional spring rate, expressed in terms of the primitive parameters of the system (calibration force and linear displacement sensor voltage output), is 0.0192 μN/mV. It has an equivalent value of 0.140 Nm/rad when written in natural units. The manufacturer of the pivots tabulates a value of $0.092 \pm 10\%$ Nm/rad at zero load, that is, $0.180 \pm 10\%$ Nm/rad for the pair of pivots. The discrepancy with our calibration can be caused by a deficiency in our pivots, or to the fact that when the pivots are rigidly connected to the frame and the arm of the balance they are loaded with significant torques of opposite signs. We calibrated the balance at the beginning and the end of each measurement session: the calibrations were basically indistinguishable, even when measured on different days, with different thruster weights, and with different thrust stand interfaces (i.e., power and pressure lines).

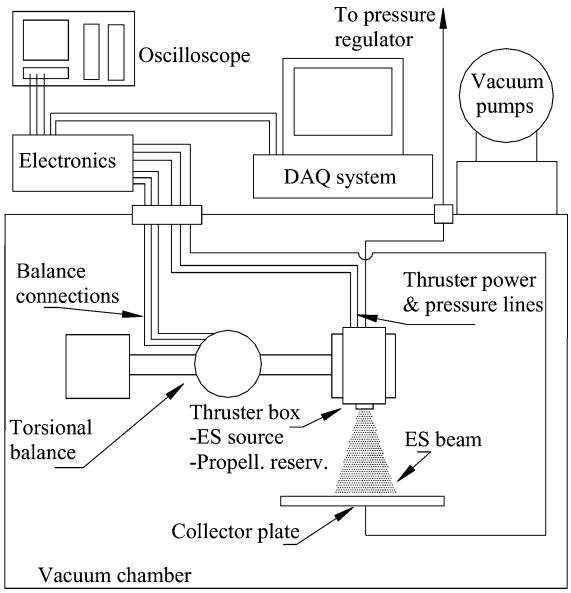

Fig. 1 Sketch of the experimental setup.

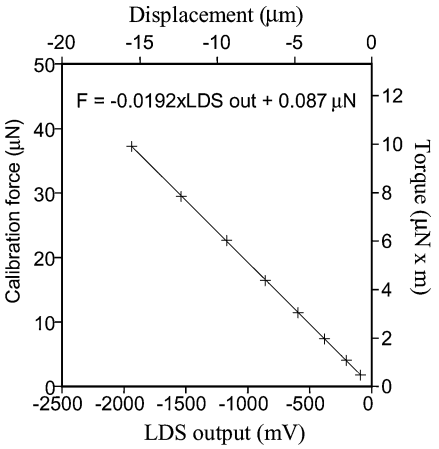

Fig. 2 Steady-state calibration of the balance.

Thrust Characterization

The six-emitter electrospray source can perform along a considerable thrust range by varying either the acceleration voltage or the propellant mass flow rate. This is exemplified in Fig. 3, in which only the acceleration voltage is modified. The flow rate of propellant is kept constant at an estimated value of 4.5×10^{-9} kg/s. (Although the flow rate was not measured, an estimate is readily computed from the pressure drop along the fluid path, its geometry, and the viscosity and density of the propellant.) Because the beam current is mostly a function of the propellant flow rate and its physical properties, it remains approximately constant during the experimental run (except when the thruster is turned off). Figure 3 shows the signals associated with the emitter voltage, the electrospray beam current, and the balance output, as a function of time. The measuring procedure is as follows: the electrospray source is initially in operation ($Vn = 2.07$ kV, $In = 2.78$ μA), yielding a thrust of 7.89 μN. The offset of the balance signal is determined by turning off the electrospray source (the emitter voltage is lowered and made equal to the voltage of the extractor; see voltage and current curves at $t \sim 46$ s), which causes the balance signal to relax to its equilibrium

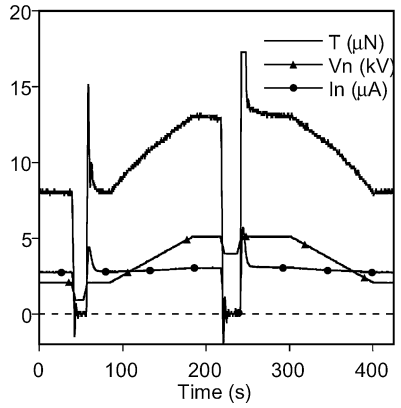

Fig. 3 Thrust output for constant beam current (In = 2.78 μA) and varying acceleration voltage.

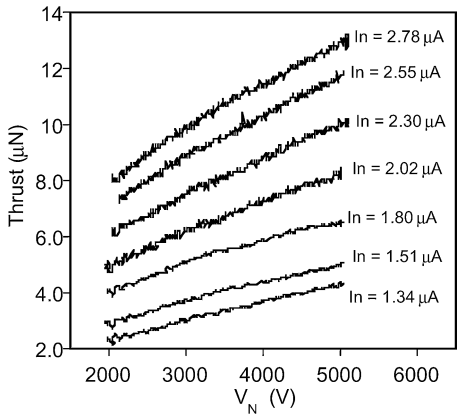

Fig. 4 Covering the 2.33–12.9 μN thrust range by varying Vn and In.

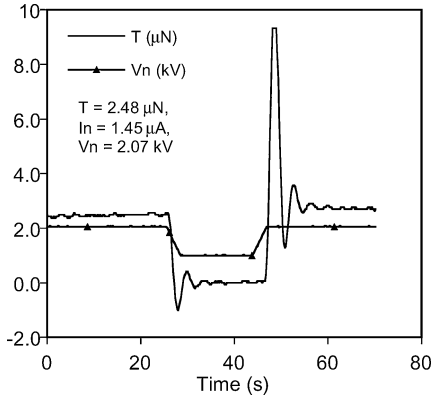

Fig. 5 Accurate measurement of a $\{T, In, Vn\}$ point.

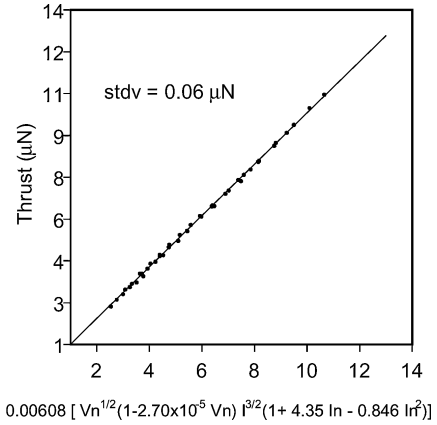

Fig. 6 Numerical fitting of the $T(In, Vn)$ data.

position. Once the equilibrium position is determined, the electrospray source is turned back on. It takes a few seconds for the thrust to reach its steady-state value because the extra amount of propellant surrounding the emitters, resulting from the instant during which the electrospray power was turned off, needs to be fully extracted. During this transient, the flow rate of electrosprayed propellant is larger than during steady-state performance, and the thrust is accordingly higher. The acceleration voltage is then ramped up, which results in an increase of the thrust, until a value of 5.07 kV (12.9 μN) is reached. The equilibrium position of the balance is determined again by shutting down the electrospray source (the emitter voltage is lowered and made equal to the voltage of the extractor), and finally the acceleration voltage is ramped down to the initial value of 2.07 kV.

The thrust data from several runs similar to that of Fig. 3 are combined in Fig. 4, where we plot T vs Vn using the beam current as a parameter. The noisy aspect of these curves is not caused by the thrust noise of the colloid beam, but it is the result of the oscillations of the balance at its natural frequency, $f_n \sim 0.25$ Hz., and which are mostly induced by spurious sources of external noise. Figure 4 demonstrates that the thrust can be varied continuously in the range 2.33–12.9 μN by adjusting the flow rate and Vn. The thrust step size is determined by the resolution with which the acceleration voltage and the propellant feed are applied, typically fixed by the resolution of the digital components of the system. Note that the thruster was not tested up to the 20-μN level required by the ST7 mission: this could be accomplished by further increasing the propellant flow rate or the acceleration voltage. We did not use larger flow rates in these experiments because the orifices of the extractor and accelerator plates were not big enough to allow the passage of broader beams. (The solid angle of each emitter's conical beam increases with the propellant flow rate.) This can be easily solved by increasing the diameter of the orifices. Voltage breakdowns in the balance feedthroughs prevented increasing the emitter voltage beyond 5 kV.

An important issue is the predictability, or resolution, with which a command on a thrust value can be executed. This problem involves guessing a pair $\{In, Vn\}$ appropriated for the thrust commanded and computing the difference between the actual and the requested T values. This question can be answered by taking accurate thrust measurements at different $\{In, Vn\}$ pairs and fitting these data to a model function $T(In, Vn)$. Then, the standard deviation of the fitting can be used as a good estimate of the resolution. Figure 5 illustrates an accurate thrust measurement: we record both the response of the balance to a given $\{In, Vn\}$ excitation and the equilibrium position of the balance (thruster turned off), consecutively. Note that the T signal is actually the output in volts of the linear displacement sensor multiplied by the calibration in Fig. 2, and thus it is equivalent to thrust only for steady state. These single point $\{T, In, Vn\}$ measurements are used, rather than the data of Fig. 4, to reduce the negative effects of balance oscillations (by averaging the signal during several natural periods of the balance) and shifts of the equilibrium position (by minimizing the time of the measurement) caused by spurious tilting of the balance. Figure 6 shows a $T(In, Vn)$ fitting obtained with 42 of these points taken in the 3–11 μN, 2.07–4.06 kV, and 1.45–2.81 μA range. The experimental data are well fitted by the formula:

$$T = 0.00608\left[V_n^{\frac{1}{2}}\left(1 - 2.70 \times 10^{-5} V_n\right) I_n^{\frac{3}{2}}\left(1 + 4.35 I_n - 0.846 I_n^2\right)\right] \tag{1}$$

where thrust, needle voltage, and beam current are expressed in micro Newtons, volts, and microamperes. The dependence of Eq. (1) on the beam current is based on the scaling law for the electrospray current[14]:

$$I_n = f(K, \gamma, \varepsilon) Q^{\frac{1}{2}} \tag{2}$$

where f is a function of physical properties of the propellant. This scaling law makes it possible to compute an average specific charge for the electrospray droplets:

$$\langle q/m \rangle = I_n/\rho Q = f^2(K, \gamma, \varepsilon)\Big/\rho I_n \tag{3}$$

which is used together with the definition of thrust in terms of the beam mass flow rate and the droplet velocity (given by the specific charge and the acceleration voltage) to compute the main dependence of the thrust on the beam current and acceleration voltage[9]:

$$T = g(K, \gamma, \varepsilon, \rho) V_a^{\frac{1}{2}} I_n^{\frac{3}{2}} \tag{4}$$

Note that Eq. (4) differs from the actual fitting (1) in the use of the emitter voltage, rather than the acceleration voltage, as well as in the polynomial correction in terms of In and Vn. The acceleration voltage for these electrosprays is several hundred volts smaller than the emitter voltage typically some 200 V are spent in the formation of the cone-jet and droplets, and also a fraction of the available potential energy is transformed into radial velocity of the droplets. This uncertainty, together with the use of the approximate scaling law (2) and the average specific charge, motivates the use of the readily available emitter voltage and polynomial corrections to fit the $T(In, Vn)$ data. Finally, note that the standard deviation of the fitting (1) is 0.06 μN. If only the emitter voltage is allowed to vary at constant propellant flow rate, we obtain fittings with typical standard deviations of 0.02 μN. At these nanoNewton levels, it is likely that the standard deviation is mostly determined by the resolution with which we are measuring the output of the balance In and Vn, rather than by the natural variation of the actual $T(In, Vn)$ function.

The measurement of the thrust noise figure down to the level required by the DRS-ST7 mission, 0.1 μN/$\sqrt{}$(Hz) in the 1–30 mHz bandwidth, is surely the most challenging task. Because the intrinsic noise of the balance output sets a lower limit beyond which the thrust noise of the electrospray source cannot be measured, we recorded the motion of the balance with both the thruster turned on and off. These measurements are shown in Fig. 7, in the form of two 10,000-s. series. They were taken on consecutive days, under conditions that minimized the influence of external noise sources. Thrust values are referred to the position of the colloid thruster (lever arm of 0.254 m). The average thrust produced by the electrospray beam has been subtracted from its curve to facilitate the comparison between signals. Note that the drift of the balance position is larger in the case of the blank or "thruster-off" curve, which indicates that the drift depends on external noise sources and is not linked to the evolution of the thrust generated by the electrospray source.

Figure 8 shows the noise spectra of the two series in Fig. 7. The time span of the measurements makes it possible to compute the power spectrum down to the low frequencies of interest for the ST7 mission. We have used the following procedures to compute the noise spectra: they are based on the power spectrum

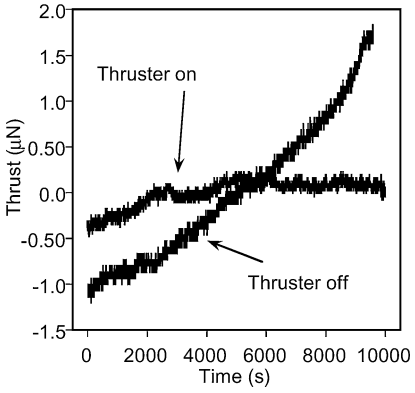

Fig. 7 10,000-s recordings of the balance output when the colloid thruster is on and off.

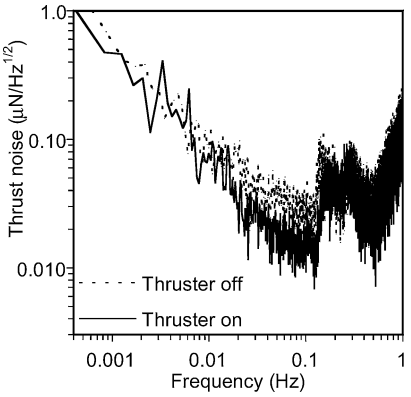

Fig. 8 Noise spectra of the data in Fig. 7.

density per unit time of the thrust; in order to reduce the variance of the periodogram estimation, the original series of sampled points were partitioned into four segments, the power spectral density for each segment was computed, and the resulting periodogram estimates were averaged at each frequency[15]; and previously, the linear trend of the original data was subtracted off each segment. Note that the noise spectrum of the thrust generated by the electrospray source is virtually indistinguishable from, or lower than, the intrinsic noise of the balance. Therefore, most the of noise in the "thruster-on" spectrum has to be caused by sources other than the thrust itself, and the balance will have to be further improved to measure the precise thrust noise spectrum. Nevertheless, the spectra in this figure are significant because, although they do not give the thrust noise figure, they prove that it is smaller than 0.1 μN/$\sqrt{}$(Hz) in the 7–1 Hz bandwidth, which is in itself an important result.

Time-of-Flight vs Torsional-Balance Measurements

Traditionally, the time-of-flight technique has been used to measure the thrust generated by colloid thrusters. The easiness of measuring the relatively high values of the beam current with moderately fast electronics, inexpensive high-voltage switches, and the difficulty of operating a thrust stand at the microNewton level, make time of flight the diagnostics of choice for colloid thrusters. The time-of-flight spectrum gives the velocity distribution of the electrospray beam, and, if the acceleration voltage of these particles is known, this velocity distribution can be converted into the kernel of integrals giving its thrust and mass flow rate.

We have compared the thrust values obtained with both the time-of-flight technique and the torsional balance, mainly to validate the former. In an attempt to improve the comparison, the two measurements were taken simultaneously for each $\{T, In, Vn\}$ state. We followed the following procedure: while the six-emitter electrospray source was turned on and generating a given thrust, its operation would be suddenly interrupted during a brief instant (typically 50 ms) and the time of flight of the beam recorded. Then, the electrospray would be turned off for a longer time to determine the equilibrium position of the balance, and hence the thrust of the beam, just as we showed in the preceding section. In these experiments we set up the high-voltage dc to dc converters powering the electrospray source, and the high-voltage switch needed for the fast interruption of the spray, inside the aluminum box housing the thruster. The remaining experimental conditions are essentially the same as those described before.

Figure 9 shows a time-of-flight spectrum. The curve is the current sensed by the electrometer at the collector plate as a function of the arrival time. The origin of time coincides with the interruption of the spray. Note the existence of both ions and droplets in the spectrum. The ion population is centered around $t = 13$ μs, while the droplets appear around $t = 77$ μs. The voltage of the emitter was 1.86 kV, and a single representative electrospraying voltage loss for all particles, 160 V, was used to compute the acceleration voltage (i.e., $Va = 1.70$ kV). The thrust and mass flow rate of the beam are

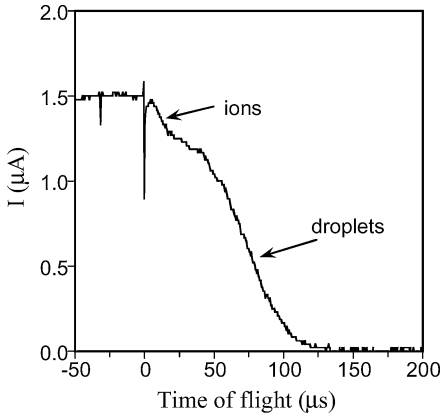

Fig. 9 Typical time-of-flight spectrum of the electrospray beam.

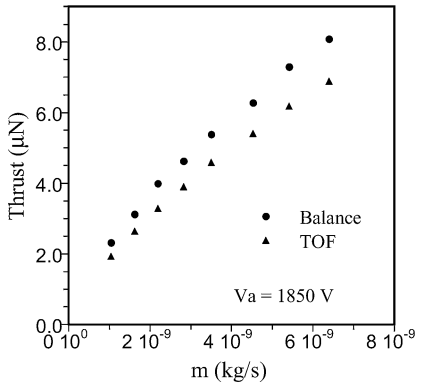

Fig. 10 Comparison of the thrust values measured with the torsional balance and the time-of-flight technique.

given by the integrals[9]

$$T = \int_0^\infty \frac{2Va(t)}{L} t I' \, \mathrm{d}t \tag{5}$$

$$\dot{m} = \int_0^\infty \frac{2Va(t)}{L^2} t^2 I' \, \mathrm{d}t \tag{6}$$

In these equations we have used the simplifying assumption that the specific charge and acceleration voltage of a beam particle are functions of its time of flight only. It is also assumed that the radial velocity of the beam particles is generated by space charge forces, rather than by the acceleration voltage. Within the uncertainties associated with other parameters in the calculation, the flight path of the beam is identified with the distance between collector plate and accelerator electrode, $L = 0.127$ m. The actual distribution of acceleration voltages $Va(t)$ is approximated by a constant value. Figure 10 shows the thrust values obtained with both techniques. The mass flow rates in the abscissa axis were computed with Eq. (6). The average difference between pairs of thrust values is 15%, that is, the uncertainties associated with the time-of-flight technique translate into a systematic error. Although the partial conversion of acceleration voltage into droplet radial kinetic energy is a possible source of error, it does not appear to be the major factor: its distortion of the thrust estimate should augment with the mass flow rate of the beam, because of increasing beam divergence. But the difference between the time-of-flight thrust estimate and the balance measurement in Fig. 10 oscillates around 15%, without a mass flow rate trend. Also, this source of error should cause an overestimate of the thrust, which is the opposite of what Fig. 10 shows. The major sources of error are probably the estimate for the voltage losses with its effect on the acceleration voltage and the oversimplification brought by the use of the time of flight as the only independent variable in the integral for the thrust. A rigorous measurement of the thrust and mass flow rate based on the properties of the beam requires the spatial characterization of the velocity, specific charge and charge distributions of the beam, which cannot be accomplished with a time-of-flight apparatus featuring a single collector.

Our opinion on the relevance of the time-of-flight technique to colloid thrusters is that it is an excellent tool to study the structure and general properties of electrospray beams and, if carefully used, can also quantify with relative accuracy thrust and mass flow rates. In the absence of a balance, we recommend taking an independent measurement of the mass flow rate (e.g., using an flowmeter in line with the propellant feed system) to verify the accuracy of the value given by Eq. (6), which also serves as a confirmation of the thrust measurement. However, if a more detailed characterization of the thrust is required (e.g., higher measurement accuracy or the determination of thrust noise), a good performing balance is the only option.

Conclusion

We have characterized, using a torsional balance, the thrust produced by an electrospray source down to the stringent specifications of the NASA's ST7-DRS mission. We have proved that the six-emitter colloid thruster generates thrust continuously from 2.33–12.9 μN, while operating in the 2.07–5.07 kV emitter voltage and 1.34–2.78 μA beam current ranges. The 20-μN level required by the ST7-DRS program can be reached by further increasing the acceleration voltage or the beam current. A functional fitting of the $\{T, Vn, In\}$ experimental data allows the generating of a given thrust value with a 0.06-μN error margin by selecting the appropriate emitter voltage and beam current. This resolution is further improved to 0.02 μN if the emitter voltage is varied at constant propellant flow rate. Although we cannot measure the exact thrust noise figure of the colloid thruster, we have demonstrated that it is below 0.1 $\mu\mathrm{N}/\sqrt{(\mathrm{Hz})}$ in the 7 mHz–1 Hz bandwidth, and we plan to improve the measuring technique to confirm directly the ST7-DRS noise requirement down to 1 mHz. These results indicate that colloid thrusters can deliver the propulsion specifications of missions like ST7-DRS and laser interferometer space antenna (LISA), for which the capability for precision spacecraft position control is paramount.

Although the accuracy of the thrust values obtained with the time-of-flight technique is inferior to the more direct balance measurement, the comparison between the results of both methods supports the use of the former for less demanding characterizations of colloid thrusters. When emphasis is placed on measurement accuracy, or when obtaining the noise figure of the thrust is required, the use of a thrust stand is the best, if not only option.

Acknowledgments

This research was funded by the NASA's New Millennium Space Technology 7 demonstration program, managed by the Jet Propulsion Laboratory (JPC), managed by the California Institute of Technology. We greatly acknowledge the support given by the managers of this project, W. M. Folkner and G. K. Man (JPL). We also thank the support of V. Hruby, the manager of the colloid thruster program at Busek.

References

[1]Krohn, V. E., "Liquid Metal Droplets for Heavy Particle Propulsion," *Progress in Astronautics and Rocketry*, Vol. 5, edited by David B. Langmuir, Ernst Stuhlinger, and J. M. Sellen, Jr., A. C. Press, New York, 1961, pp. 73–80.

[2]Kidd, P. W., and Shelton, H., "Life Test (4350 hrs.) of an Advanced Colloid Thruster Module," AIAA Paper 73-1078, Nov. 1973.

[3]Huberman, M. N., and Rosen, S. G., "Advanced High-Thrust Colloid Sources," *Journal of Spacecraft and Rockets*, Vol. 11, No. 7, 1974, pp. 475–480.

[4]Mueller, J., "Thruster Options for Microspacecraft: a Review and Evaluation of State-of-the-Art and Emerging Technologies," *Micropropulsion for Small Spacecraft*, edited by M. M. Micci and A. D. Ketsdever, Progress in Astronautics and Aeronautics, Vol. 187, AIAA, Reston, VA, 2000, pp. 45–137.

[5]Mazanek, D. D., Kumar, R. R., Seywald, H., and Qu, M., "GRACE Mission Design: Impact of Uncertainties in Disturbance Environment and Satellite Force Models," American Astronautical Society, Paper 00-163, Jan.

2000; also "Gravity Measurement: Amazing Grace," News Feature, *Nature*, Vol. 416, March 2002, pp. 10–11.

[6]Folkner, W. M., Buchman, S., Byer, R. L., DeBra, D., Dennehy, C. J., Gamero-Castaño, M., Hanson, J., Hruby, V., Keiser, G. M., Kuhnert, A., Markley, F. L., Houghton, M., Maghami, P., Miller, D., Prakash, S., and Spero, R., "Disturbance Reduction System: Testing Technology for Precision Formation Control," *Proceeding of Society of Photo-Optical Instrumentation Engineers*, Vol. 4860, The International Society for Optical Engineering, Waikoloa, HI, Aug. 2002, pp. 221–228.

[7]Cash, W., Shipley, A., Osterman, S., and Joy, M., "Laboratory Detection of X-ray Fringes with a Grazing-Incidence Interferometer," *Nature*, Vol. 407, Sept. 2000, pp. 160–162; also "Imaging Black Holes," News and Views, *Nature*, Vol. 407, No. 6801, Sept. 2000, pp. 146, 147.

[8]Hanson, J., Keiser, G. M., Buchman, S., Byer, R. L., Folkner, W. M., Hruby, V., and Gamero-Castaño, M., "Disturbance Reduction System for Testing Technology for Drag-free Operation," *Proceeding of Society of Photo-Optical Instrumentation Engineers*, Vol. 4856, The International Society for Optical Engineering, Waikoloa, HI, Aug. 2002, pp. 9–18.

[9]Gamero-Castaño, M., and Hruby, V., "Electrospray as a Source of Nanoparticles for Efficient Colloid Thrusters," *Journal of Propulsion and Power*, Vol. 17, No. 5, 2001, pp. 977–987.

[10]Gamero-Castaño, M., and Hruby, V., "Characterization of a Colloid Thruster Performing in the Micro-Newton Thrust Range," International Electric Propulsion Conference, Paper IEPC-01-282, Oct. 2001.

[11]Gamero-Castaño, M., Hruby, V., and Martínez-Sánchez, M., "A Torsional Balance that Resolves Sub-Micro-Newton Forces," International Electric Propulsion Conference, Paper IEPC-01-235, Oct. 2001.

[12]Gamero-Castaño, M., "A Torsional Balance for the Characterization of Micro Newton Thrusters," *Review of Scientific Instruments*, Vol. 74, No. 10, Oct. 2003, pp. 4509–4514.

[13]McEwen, A. B., Ngo, H. L., LeCompte, K., and Goldman, J. L., "Electrochemical Properties of ImidazoliumSalt Electrolytes for Electrochemical Capacitor Applications," *Journal of the Electrochemical Society*, Vol. 146, No. 5, 1999, pp. 1687–1695.

[14]Fernández de la Mora, J., and Loscertales, I. G., "The Current Emitted by Highly Conducting Taylor Cones," *Journal of Fluid Mechanics*, Vol. 260, Feb. 1994, pp. 155–184.

[15]Press, W. H., Teukolsky, S. A., Vetterling, W. T., and Flannery, B. P., *Numerical Recipes in C*, 2nd ed., Cambridge Univ. Press, New York, 1999, pp. 496–500, 549–552.